Astrophysics and Space Science
DOI 10.1007/s●●●●●-●●●-●●●●-●

First Stars. II. Evolution with mass loss

D. Bahena[1] **• P. Hadrava**[1]

arXiv:1110.4478v1 [astro-ph.SR] 20 Oct 2011

© Springer-Verlag ●●●●

Abstract The first stars are assumed to be predominantly massive. Although, due to the low initial abundances of heavy elements the line-driven stellar winds are supposed to be inefficient in the first stars, these stars may loose a significant amount of their initial mass by other mechanisms. In this work, we study the evolution with a prescribed mass loss rate of very massive, galactic and pregalactic, Population III stars, with initial metallicities $Z = 10^{-6}$ and $Z = 10^{-9}$, respectively, and initial masses 100, 120, 150, 200, and 250 $M_\odot$ during the hydrogen and helium burning phases. The evolution of these stars depends on their initial mass, metallicity and the mass loss rate. Low metallicity stars are hotter, compact and luminous, and they are shifted to the blue upper part in the Hertzprung-Russell diagram. With mass loss these stars provide an efficient mixing of nucleosynthetic products, and depending on the He-core mass their final fate could be either pair-instability supernovae or energetic hypernovae. These stars contributed to the reionization of the universe and its enrichment with heavy elements, which influences the subsequent star formation properties.

Keywords first stars, stars: models, evolution, mass loss

1 Introduction

It is widely accepted that the so called Population III stars, i.e. the first stars formed from the primordial gas with an extremely low metallicity, have played an important role in the evolution of the universe. The first stars are assumed to be predominantly very massive and they were responsible for reionization of the universe and its enrichment by heavy elements.

The formation of the first stars and hence also their Initial Mass Function (IMF) is significantly influenced by the low metallicity of the protostellar material. Due to its low opacity, its gravitational attraction can not be effectively opposed by radiative pressure and the continuing accretion gives rise to more massive stars.

Numerical hydrodynamic simulations of star formation generally confirm the tendency to higher masses of the first stars, although quantitatively the results differ considerably.

Bromm and Larson (2004) found the masses of the first stars between 10^2 and $10^3 M_\odot$, Omukai and Palla (2003) followed the evolution of accreting protostars and found $\sim 600\,M_\odot$ as the upper limit for massive stars. According to Abel et al. (2002), the final masses are uncertain because a single molecular protostar seed of $\sim 1 M_\odot$ at the centre of a $\sim 100\,M_\odot$ core of a protogalaxy is formed. The cores may fragment into clusters of massive (MS) or very massive stars (VMS). Nakamura et al. (1999) found $3\,M_\odot$ as the mass of the first stars which may grow up to $\sim 16\,M_\odot$ by the accretion. The IMF of Population III could thus be bimodal with peaks at $\sim 1-2\,M_\odot$ and $\sim 10^2\,M_\odot$ (Nakamura and Umemura 2001). Tumlinson et al. (2004) defined *strong VMS hypothesis* ("The first generation were exclusively VMS") and the *weak VMS hypothesis* ("The first generation included VMS in addition to MS with $M \lesssim 50\,M_\odot$").

The structure, evolution and properties of the first stars have been modelled in several studies including the Paper I of this series (Bahena and Klapp 2010). The results showed that the Population III stars are

---

D. Bahena

P. Hadrava

[1] Astronomical Institute of the Academy of Sciences,
Boční II 1401, 14131 Praha 4, Czech Republic.
e-mail: bahen@hotmail.com, had@sunstel.asu.cas.cz

smaller but more luminous and hotter than the normal metal-richer Population I an II stars of equal masses.

The massive luminous normal stars have a high mass loss mainly due to the stellar wind driven by radiative pressure in lines of metals (Castor et al. 1975, the so called CAK-wind). This process cannot take place in the metal-free stars (Bromm and Loeb 2003). This is why practically all models of first-stars evolution have neglected completely the mass loss.

Several recent studies, however, revealed that even in the absence of CAK-wind there may occur a considerable mass loss due to different alternative processes.

A reliable quantitative theory of the mass loss rate in the Population III stars is still missing, but it is of great interest to investigate the possible consequences of the mass loss on the properties of these stars. For this purpose we extend hereby our calculations of the conservative case of the first-stars evolution in Paper I assuming a mass loss rate given by an ad-hoc parametrization.

This work is organized as follows: In Sect. 2 the mass loss mechanisms are reviewed. In Sect. 3 we describe the initial conditions and results of the computed models, the main physical variables and their properties. Then, in Sect. 4 we discuss our results in comparison with the conservative case. Finally, in Sect. 5 we summarize the conclusions.

2 Mass Loss Mechanisms

The mass loss in stars of Population I and II has been studied both theoretically and observationally. However, an extrapolation of the results to stars of Population III is questionable due to very different physical properties of both the interiors as well as the atmospheres of the stars.

Regarding the short lifetimes of the massive first stars, their mass loss rates have thus to be estimated from the theoretical considerations and only an indirect evidence can be gained from observations of later generations of stars. E.g., the abundances of elements and isotopes observed in metal-poor halo stars (Beers and Christlieb 2005) suggest that these stars were formed from an interstellar matter enriched by mass lost during the H- and He- burning in the first stars rather than by debris of pair-instability supernovae (SNe) expected to be the final stage of the first VMS evolution (Hirschi et al. 2008; Cescutti and Chiappini 2010).

2.1 Stellar winds

The mass loss via stellar winds influences significantly the evolution of massive Population I and II stars and contributes a great deal to the enrichment of interstellar matter by heavy elements.

For cool winds of Population I red giants on the RGB Reimers (1975, 1977) found an empirical relation giving the mass loss rate as

$$\dot{M} \sim \frac{L}{gR} \sim \frac{LR}{M} \,, \tag{1}$$

where L, R, M and g are the luminosity, radius, mass and surface gravity of the star. Schröder and Cuntz (2005) obtained a semi-empirical generalization of the Reimers' relation.

The stellar winds are significantly enhanced at the early-type stars by radiative pressure either in continuum or especially in lines. The dependence of the mass loss rate due to CAK-wind on the metallicity has been scaled by the relation

$$\dot{M} \sim Z^{\zeta} \,, \tag{2}$$

where the exponent varies between $0.5 - 0.8$ for $0.01 \leq Z/Z_{\odot} \leq 1.0$ (Leitherer et al. 1992; Vink et al. 1999, 2000, 2001). However, Kudritzki (2002) has found that this relation breaks down below a certain threshold of the metallicity.

Krtička and Kubát (2006, 2009); Krtička et al. (2010b) have studied line-driven winds from the first stars. They showed that weak stellar winds may be due to absorption in lines of CNO elements carried by mixing from the interiors to the atmospheres of the stars.

2.2 Rotation

The Population III stars are supposed to be faster rotators than the stars with higher metallicity (Maeder et al. 1999; Meynet et al. 2006b). The numerical hydrodynamic models of star-formation by Stacy et al. (2011) also indicate high angular momenta of the first stars, what influences their structure, evolution and final fate. The effects of rotation on the structure and evolution of massive stars were studied by the Geneva Group (Meynet and Maeder 1997; Maeder 1998; Maeder and Meynet 2001; Meynet and Maeder 2000, 2002). The rotation may increase the mass loss by several processes:

1. The rotational mixing enhances the atmospheres with heavier elements which facilitate the radiatively driven winds (Lamers et al. 1995).
2. The gravitational darkening enhances the radiative flux and the mass loss on poles of the rotationally

oblate stars while reducing the angular-momentum loss (Maeder and Desjacques 2001; Dwarkadas and Owocki 2002).

3. The centrifugal force reduces the gravity on the equator. When approaching the critical rotation, the decretion disks are formed through which the angular momentum and significant amount of mass is lost (Krtička et al. 2010a, 2011).

2.3 Pulsation

The pulsational instability of very massive stars might contribute somewhat to the total mass loss rate although it is not clear what the contribution will be. Cool supergiants do indeed have winds which are initiated by pulsations, but then further support, such as radiative force on the dust grains, is needed to sustain a significant outflow.

The stability of very massive stars was analyzed and compared with metal enriched stars by Baraffe et al. (2001). Mass loss was not taken into account because they assumed it to be negligible for zero-metallicity stars. A linear non-adiabatic analysis was carried out. In their analysis, they considered that the stars stabilize as soon as they evolve from the ZAMS, then one can expect decreasing mass loss rates along the main sequence. This is, pulsations do not lead to significant mass loss on the main sequence. For their calculations they used the so called *flux-freezing convective theory* that assumes that perturbation in the luminosity is only given by the radiative luminosity. However, the stability properties of the models could change if convection is properly taken into account (Klapp et al. 2005).

Thus, the issue of whether very massive stars could be vibrationally unstable to pulsation and induce pulsationally driven mass loss is still open. The contribution of pulsation to mass loss remains uncertain.

2.4 Other mechanisms

Smith and Owocki (2006) suggested that the mass loss during the evolution of Population III stars may be dominated by optically thick, continuum-driven outbursts or hydrodynamical explosions, similarly as in the very massive Luminous Blue Variable (LBV) stars and η Car in particular. Unlike the steady line-driven winds, this mechanism, investigated also, e.g., by van Marle et al. (2008a,b), is insensitive to metallicity but requires a high, nearly Eddington luminosity, close to which the mass loss rates of the wind highly increase (Kudritzki 2002; Gräfener and Hamann 2002; Vink et al. 2011). This condition is well satisfied by the first stars owing to their high masses and luminosities.

The role of magnetic fields in activity of late-type stars and their winds is generally known. The growing observational evidence of magnetic fields in early-type stars (e.g. Be-stars) suggests that they could also be present in the first stars and consequently influence their winds or mass loss via their decretion disks (cf., e.g., Puls et al. 2008; ud-Doula et al. 2008, and references therein). However, it is not clear whether there was a magnetic field in the interstellar medium in the early universe.

Finally, because the first stars were also created in binaries and multiple systems, they could be subjected to mass-exchange, mass loss from their systems and enhancement of their winds by tidal forces from companion stars as it is theoretically well understood and observationally confirmed for the present generations of stars.

Motivated by these studies we explore a scenario for the evolution of very massive and low-metallicity Population III mass losing stars.

3 Evolutionary Models at Low Metallicity

3.1 Input physics and initial conditions

In agreement with Castellani (2000) we take as the Population III stars all the stellar objects with metallicity below a not yet well defined upper limit between $Z = 10^{-10}$ and 10^{-6}. Depending on their metallicity we distinguish between galactic and pregalactic stars, the former with metallicity $Z = 10^{-6}$, and the later with $Z = 10^{-9}$, both considered as lower metallicity stars, but not zero-metallicity stars.

The concept of critical metallicity has been used to characterize the transition between Population III and Population II star formation modes (Omukai 2001; Bromm et al. 2001; Schneider et al. 2002, 2003; Mackey et al. 2003; Bromm and Larson 2004).

Our evolutionary models for both galactic and pregalactic Population III stars have been calculated by using a stellar code described in Paper I by Bahena and Klapp (2010). These models assume the standard quasistatic non-rotating configuration of the stars. A semiconvection treatment for convective transport of energy has been used. In addition to the assumptions on the underlying physics used in Paper I, we include now also a mass loss parametrization.

In view of the uncertainty in the dominant mass loss process in the Population III stars, the corresponding mass loss rates and their changes with the stellar parameters as summarized in the previous Section, we have adopted a simple parametrization of the mass loss rate, based on the first relations proposed by Lucy and Solomon (1970) and Barlow and Cohen (1977) to explain the mass loss for hot luminous stars,

$$\dot{M} = NL/c^2 \ , \tag{3}$$

where L is the luminosity of the star, c is the speed of light, and N is a mass loss parameter. This parameter is taken as an average measure of the mass loss rate and it is kept constant in the course of the whole evolution. It is based on the simplifying assumption that the mass-energy output of the star in the form of non-zero rest-mass particles is proportional to its radiative output.

Different models of stellar winds give the mass loss rates in the form of power-law in luminosity with various exponents and they usually also depend on other stellar parameters. Let us note that unlike the Reimers' formula (1) corresponding to the stellar winds of late-type stars, which for chosen M gives the $\dot{M}$ proportional to R increasing for orders of magnitude for stars evolving from the main sequence to the red-giant branch, our approximation (3) intended to an unspecified mass loss mechanism varies linearly with L only, i.e. much less in the course of evolution of the star.

It can be expected that the mass loss rate is more complicated in reality, however, to get an insight into its possible effects on the stellar evolution before a proper model of the mass loss mechanism will be available we are limited to the use of such an *ad hoc* assumption. In our parametrization, the mass loss parameter $N = 100$ gives for the luminosity $L \sim 10^6 L_{\odot}$ typical for stars with mass of the order $100\, M_{\odot}$ a mass loss rate of $\dot{M} \sim 10^{-5} M_{\odot}\mathrm{yr}^{-1}$ which is able to reduce significantly the initial mass of the star during its characteristic lifetime $\tau \sim 10^6$yr. Calculations with different N values should be indicative for the way in which the evolution of massive first stars is affected by the mass loss.

To facilitate a comparison with models without mass loss the initial conditions for the models presented here have been chosen the same like in Paper I.

The chemical composition corresponding to galactic lower metallicity stars is $(X, Z = 0.765, 10^{-6})$, and for pregalactic ones $(X, Z = 0.765, 10^{-9})$ by using a value $Y = 0.235$ as a primordial helium value. The initial stellar masses have been chosen 100, 120, 150, 200, and $250\, M_{\odot}$. For the mass loss parameter we have used the values $N = 50$ and 100.

3.2 Properties of the models

The evolutionary models presented here predict the effective temperature, luminosity and other physical variables and quantities for very massive Population III mass losing stars during the hydrogen and helium burning phases, for the initial masses and mass loss parameters chosen.

Figures 1 to 4 show some physical variables during the hydrogen and helium burning for pregalactic stars with masses 100, 120, 150, 200, and 250 $M_{\odot}$, metallicity $Z = 10^{-9}$ and mass loss parameter $N = 100$.

Population III stars are hotter than their metal enriched counterparts, and their locus in the HR-diagram is shifted to the left upper part; pregalactic stars are bluer than the galactic ones.

For a given stellar mass of main-sequence stars its location in the HR-diagram depends strongly on metallicity but also on the mass loss strength. During the hydrogen burning, the higher the mass loss rate, the greater the reduction in luminosity.

Our models exhibit a high production of ionizing photons. This confirms the important cosmological consequences of the first generation of stars for the reionization of the universe.

Depending on their initial mass and the mass loss rate the final fate of our models could be as supernovae or hypernovae explosions.

a) Central density and temperature

Lower metallicity stars are denser than the enriched stars. At the beginning of the evolution, galactic and pregalactic stars have different central densities which increase with decreasing Z. The central density increases with decreasing stellar mass and it is higher for lower metallicity stars.

As the evolution goes on, the mean molecular weight increases and the density and temperature increase. During hydrogen burning, both the central density and temperature increase slowly until hydrogen is exhausted in the core.

The most massive stars, and lower metallicity stars, have higher central temperature. According to Bromm et al. (2001) the central temperature is related to the mass and radius as

$$T_{\mathrm{c}} \sim \frac{M^{1/2}}{R} \ . \tag{4}$$

For stars with $M > 100\, M_{\odot}$ the central temperature is insensitive to both mass and radius and depends upon the composition only. In the absence of metals, T_{c} is higher and the star self-generates the small amount of CNO elements needed for energy generation to support the star (Castellani 2000).

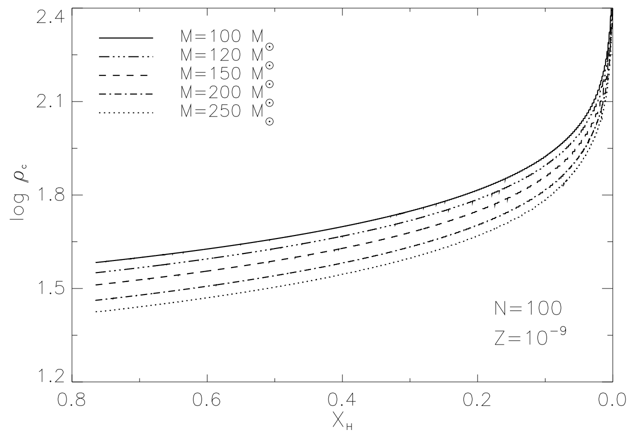

Fig. 1 Central density for $100\,M_{\odot}$ (solid line), $120\,M_{\odot}$ (dash-dot-dot-dot-dash), $150\,M_{\odot}$ (dashes), $200\,M_{\odot}$ (dash-dot-dash) and $250\,M_{\odot}$ (dots) pregalactic Population III stars with metallicity $Z = 10^{-9}$ and mass loss parameter $N = 100$ during the hydrogen burning phase.

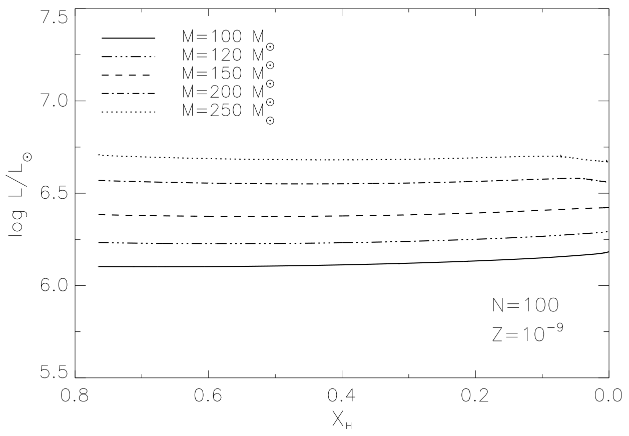

Fig. 2 Idem dito. Luminosity

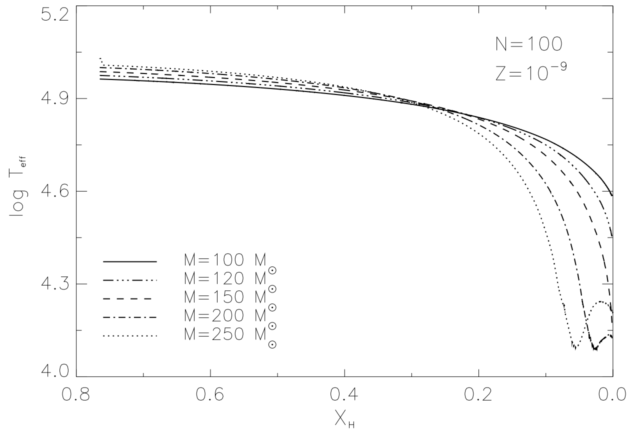

Fig. 3 Idem dito. Effective temperature

b) Effective temperature and radius

At the beginning of the main sequence, galactic stars with metallicity $Z = 10^{-6}$, and mass loss parameter $N = 50$, have an effective temperature $T_{\rm eff} = 69582$, 73416, and 75586 K for a 100, 150 and 200 $M_{\odot}$, respectively. For the same stellar masses, pregalactic stars with $Z = 10^{-9}$ have $T_{\rm eff} = 91865$, 97109, and 100090 K, respectively. Due to mass loss, the effective temperatures decrease during core hydrogen burning. At the end, these temperatures are lower than for the conservative case.

On the main sequence, 100, 150, and 200 $M_{\odot}$ galactic stars with metallicity $Z = 10^{-6}$, have initial radii $R = 7.67$, 9.54 and 11.15 $R_{\odot}$, respectively, and for pregalactic stars with $Z = 10^{-9}$, their radii are $R = 4.48$, 5.55 and 6.46 $R_{\odot}$, respectively.

With decreasing effective temperature, the radius increases. For stars evolving with high mass loss parameters, their radii at the end of the hydrogen burning increase even more.

The changes of the radius and effective temperature can be understood in terms of changes in the convective core size. To satisfy the boundary condition

$$L = \pi a c R^2 T_{\rm eff}^4 \qquad (5)$$

the effective temperature decreases with increasing radius. An expanding convective core implies a decreasing radius and increasing effective temperature.

b) Convective core size

During the hydrogen burning the convective core evolves in different ways depending on whether the stars are mass losing or not. If a star evolves with mass loss its convective core decreases continuously during

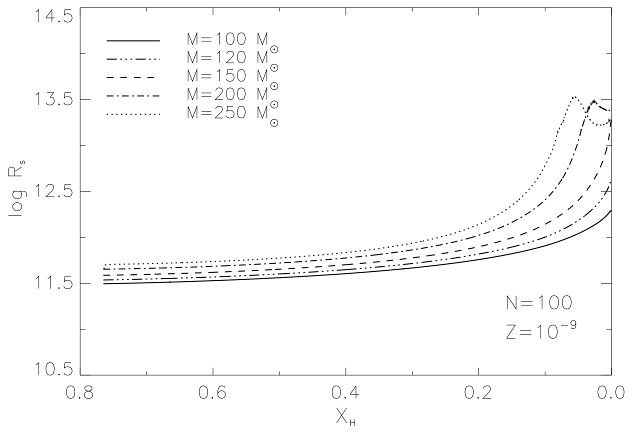

Fig. 4 Idem dito. Radius

the hydrogen burning phase. In the conservative case, a helium core is formed only at the end of hydrogen burning when the star is contracting during its transition to helium burning.

At the end of hydrogen burning, the convective core size, defined as the ratio $q_{\rm cc} = M_{\rm cc}/M$ of the convective core mass $M_{\rm cc}$ to the total stellar mass M, is larger for evolution with mass loss than for the conservative case. This is because for mass losing stars their initial mass is reduced during the evolution. Figure 5 shows the evolution of the convective core size during the hydrogen burning for pregalactic Population III stars and mass loss parameter $N = 100$.

d) Luminosity and Gamma factors

Luminosity increases or decreases during evolution with mass loss depending on the mass loss rate. The rate of decrease of the luminosity is higher for large mass loss parameters.

In Figure 6, the mass-luminosity $(M - L)$ relation is shown for $100\,M_\odot$ galactic and pregalactic Population III mass losing stars during the hydrogen burning. For low values of the mass loss parameter $N = 50$, the luminosity increases during hydrogen burning but decreases for large values of $N = 100$. This is because in VMS the opacity is mostly due to electron scattering. Then, as the evolution goes on, the opacity decreases and the mean molecular weight increases. Both of these effects contribute to an increase of luminosity which is proportional to the stellar mass. The $M - L$ relation reads

$$L \sim M^{\eta}\,, \tag{6}$$

where the value of the exponent η depends on the mass loss rate. The evolution reaches a given mass with higher luminosity, the lower the value of N is.

Figure 7 shows the Gamma factor during the core hydrogen burning, for pregalactic Population III stars with a mass loss parameter $N = 100$.

Galactic, and pregalactic Population III stars evolve during hydrogen burning near the Eddington upper luminosity limit. With and without mass loss, the ratio between the luminosity of the star and its Eddington luminosity is similar.

In Figures 8 and 9, the Gamma factor is plotted as a function of the radius showing the phase when this factor approaches to unity, during the hydrogen burning, for mass losing galactic and pregalactic stars, respectively.

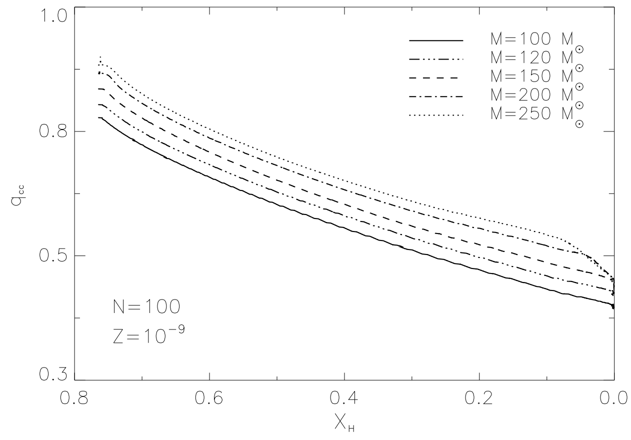

Fig. 5 Convective core size for $100\,M\odot$ (solid line), $120\,M_\odot$ (dash-dot-dot-dot-dash), $150\,M_\odot$ (dashes), $200\,M_\odot$ (dash-dot-dash) and $250\,M_\odot$ (dots) pregalactic Population III stars with metallicity $Z = 10^{-9}$ and mass loss parameter $N = 100$ during the hydrogen burning.

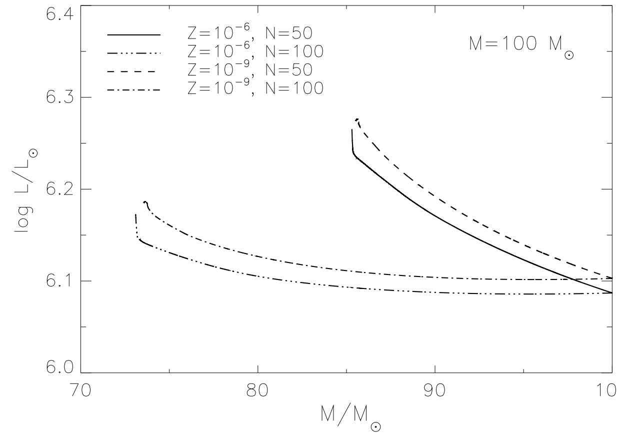

Fig. 6 Mass-luminosity relation for $100\,M_\odot$ galactic and pregalactic Population III stars with metallicity $Z = 10^{-6}$ and $Z = 10^{-9}$, respectively, and mass loss parameters $N = 50$ and $N = 100$, during the hydrogen burning.

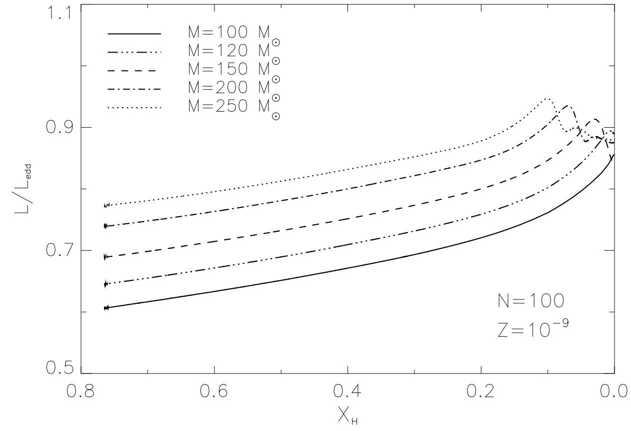

Fig. 7 The Γ factor for pregalactic Population III stars with metallicity $Z = 10^{-9}$ and mass loss parameter $N = 100$ during the hydrogen burning.

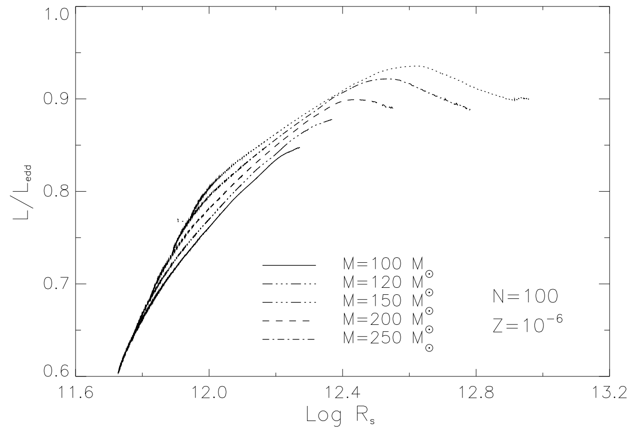

Fig. 8 The Γ factor as function of the radius for galactic Population III stars with metallicity $Z = 10^{-6}$ and mass loss parameter $N = 100$ during the hydrogen burning.

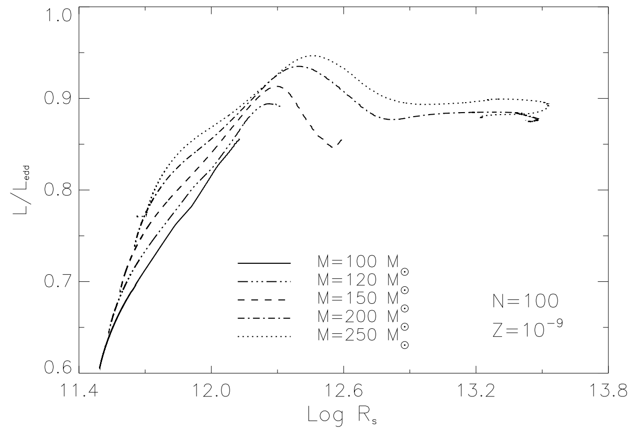

Fig. 9 Idem dito. Pregalactic Population III stars with metallicity $Z = 10^{-9}$ and mass loss parameter $N = 100$ during the hydrogen burning.

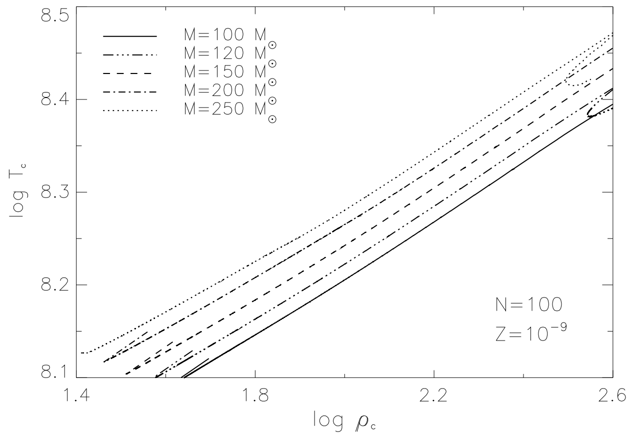

Fig. 10 $\log T - \log \rho$ plane for 100, 120, 150, 200 and $250\,M_\odot$ pregalactic Population III stars with metallicity $Z = 10^{-9}$, and mass loss parameter $N = 100$, during the hydrogen and helium burning phases.

e) $\rho - T$ plane

In the $\rho{-}T$ plane the galactic and pregalactic very massive Population III mass losing stars occupy the upper loci of a nondegenerate and nonrelativistic gas. In this zone there is an upper boundary at which pair production effects could become important. The most massive stars tend to approach to it, however, our models are below this boundary. Regarding the gas in thermodynamic equilibrium, mass losing stars studied here are dominated by radiation pressure. Fig. 10 shows the evolution of conditions in the centres of stars.

f) HR diagram

As in the conservative case, the locus of very massive Population III stars in the HR diagram is in the left upper part. Pregalactic stars are hotter than the galactic ones. The most massive stars are the most luminous. Depending upon the star's initial mass and mass loss rate, its evolution can be different.

During hydrogen burning, the luminosity of a star without mass loss increases while a helium core is formed. Then, as the star evolves, the luminosity remains almost constant while the effective temperature decreases. However, for different stars their luminosity and effective temperature decrease with decreasing mass and increasing metallicity. The luminosity is lower for mass losing stars than for stars without mass loss.

Different stars evolve with different lifetimes. Depending on the mass loss rate, both the initial hydrogen and helium burning phases take place at the blue side of the HR diagram. When the stars evolve with assumed mass loss rates they move toward the red, like in the conservative case. With and without mass loss the stars do not experience the AGB phase.

Figures 11 to 14 show evolutionary tracks in the HR diagram for 100, 120, 150, 200 and $250\,M_\odot$, for mass loss parameters $N = 50$ and $N = 100$, corresponding to galactic and pregalactic Population III stars with metallicity $Z = 10^{-6}$ and $Z = 10^{-9}$, respectively.

4 Discussion

Population III stars are defined as all metal deficient stars which share the common peculiarity of experiencing self-production of C sometimes during their H-burning evolution (Castellani 2000). That is, these stars may build-up a small fraction of C nuclei ($Z_{\rm C} \sim 10^{-10}$) via the triple-α reactions during the pre-main sequence (Cassisi and Castellani 1993).

Then, these stars produce their nuclear energy during the H-burning phase from a combination of the

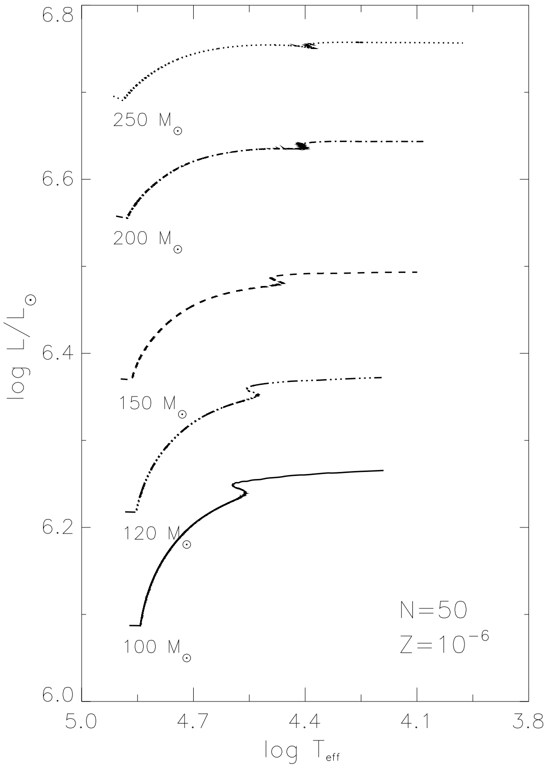

Fig. 11 Evolutionary tracks in the HR-diagram for 100, 120, 150, 200 and 250 $M_\odot$ galactic Population III stars with metallicity $Z = 10^{-6}$ and mass loss parameter $N = 50$, during the hydrogen and helium burning phases.

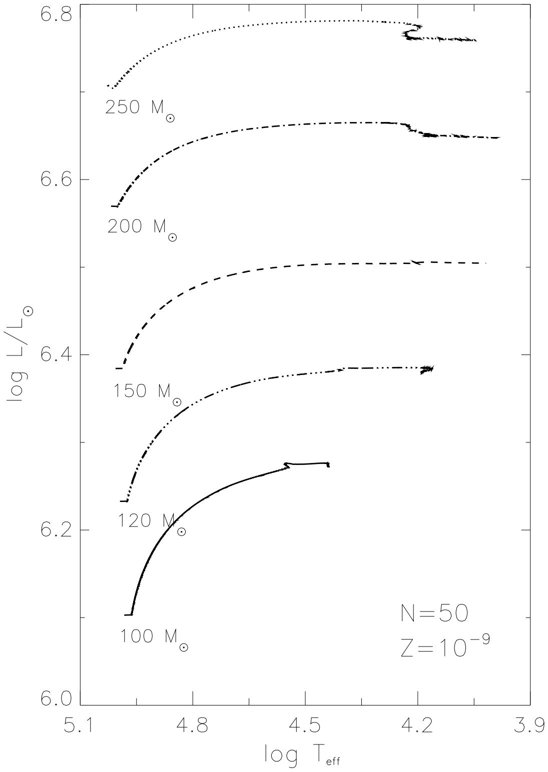

Fig. 13 Evolutionary tracks in the HR-diagram for 100, 120, 150, 200 and 250 $M_\odot$ pregalactic Population III stars, metallicity $Z = 10^{-9}$, and mass loss parameter $N = 50$, during the hydrogen and helium burning phases.

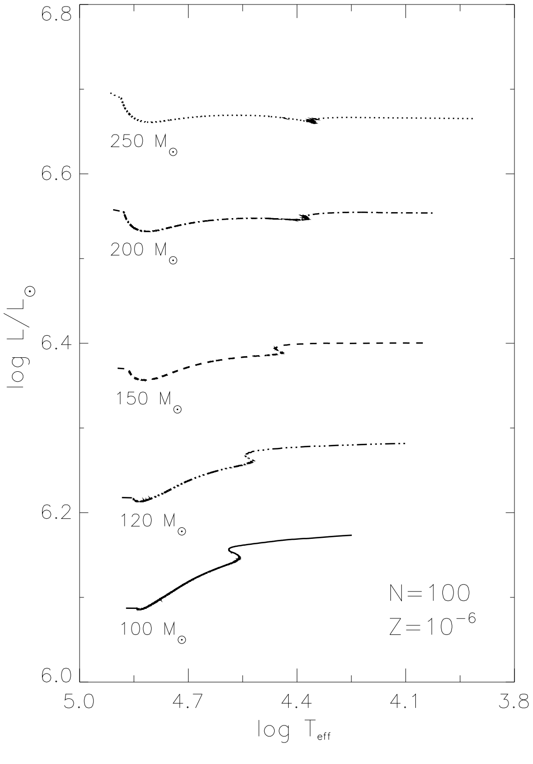

Fig. 12 Idem dito. Mass loss parameter $N = 100$.

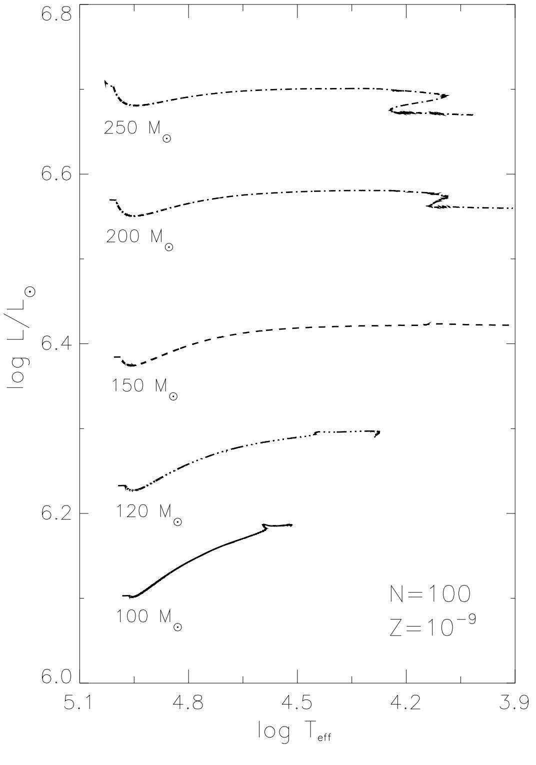

Fig. 14 Idem dito. Mass loss parameter $N = 100$.

proton-proton (pp) chain and the CNO-cycle with the small amount of C previously built. To provide the necessary luminosity, the star has to reach very high central temperatures $T_{\rm c} \sim 10^8$ K for the simultaneous occurrence of the helium burning via the 3α process. This burning produces certain amount of heavy elements to follow efficiently the CNO-cycle.

In our models, the lower is the metallicity, the sooner is activated the triple-α reaction during the main-sequence. Lower-metallicity pregalactic stars without mass loss produce higher nuclear energy via the triple-α reaction from the beginning of the main-sequence. For galactic stars contribution of this reaction is at the end of the main-sequence only. This is shown in Figure 15. For mass losing stars, the nuclear energy production via the pp-chain, CNO-cycle and 3α reaction is higher than in the conservative case, and 3α reaction starts from the beginning of the main-sequence, as it is shown in Figure 16.

As a result of lower energy-generation rate in the core, the stars maintain high central temperatures to support the stellar mass against the gravitational collapse. This high temperatures in the core and reduced opacity in their envelopes make these stars hotter and more compact than their enriched counterparts, depending on the initial stellar mass and metallicity.

The lower is the metallicity, the more compact and hotter are the stars. Table 1 shows models with 100 $M_\odot$ when they settle down on the main-sequence. A galactic star with metallicity $Z = 10^{-6}$ has a radius of 7.68 $R_\odot$, while a pregalactic star with $Z = 10^{-9}$ has 4.49 $R_\odot$ or with $Z = 10^{-10}$ it has 3.69 $R_\odot$. Concerning the effective temperature this is 69582, 91865 and 101800 K, respectively. On the ZAMS, the pregalactic lower metallicity stars are denser, hotter and slightly more luminous than galactic ones.

With effective temperatures of $T_{\rm eff} \sim 10^5$ K these stars are very efficient at producing photons capable of ionizing the hydrogen and helium (Bromm et al. 2001).

Lower metallicity stars are shifted to the blue upper part of the HR-diagram. When stars are gradually enriched with heavy elements they evolve redwards. This is shown in Figure 17 for a 100 $M_\odot$ model without a mass loss. Mass losing stars evolve reducing their mass, luminosity and effective temperature, as it is shown in Figure 18.

In our models, evolutionary tracks describe different paths on the HR-diagram depending on stellar mass and mass loss rates. Galactic and pregalactic Population III mass losing stars move from the left to the right in the upper part of this diagram. With higher mass loss rates, the luminosity and the effective temperature decreases more than in the conservative case.

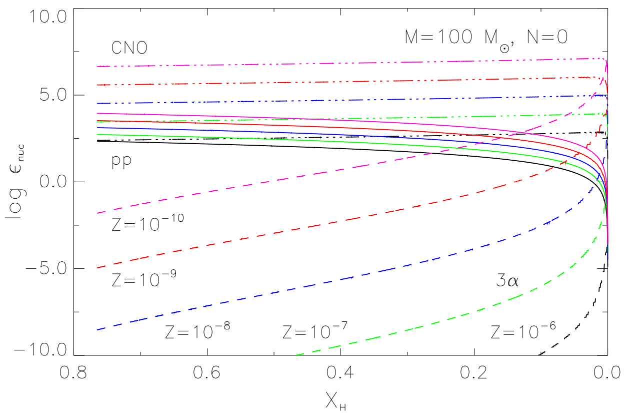

Fig. 15 Nuclear energy generation via pp-chain, CNO-cycle and 3α-reaction for galactic and pregalactic Population III stars with initial metallicity $Z = 10^{-6}$ to $Z = 10^{-10}$, without mass loss during the hydrogen burning.

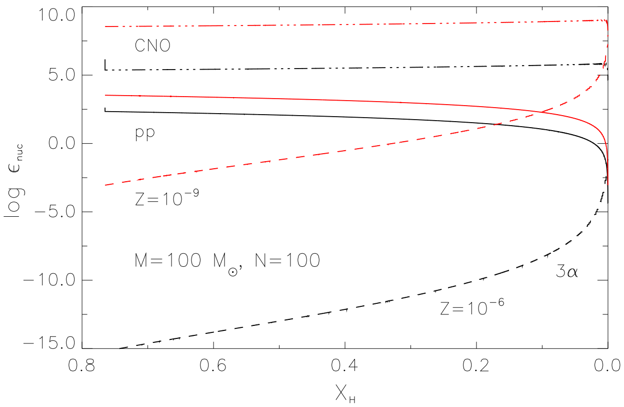

Fig. 16 Nuclear energy generation via pp-chain, CNO cycle and 3α-reaction for galactic and pregalactic Population III stars with initial metallicity $Z = 10^{-6}$ and $Z = 10^{-9}$, with mass loss during the hydrogen burning.

Table 1 Some characteristics of lower-metallicity 100 $M_\odot$ stars when settle down on the main-sequence. Models become more hotter, denser, luminous and compact, as metallicity is decreasing.

Z	log $T_{\rm c}$	log $\rho_{\rm c}$	log $\frac{L}{L_\odot}$	log $T_{\rm eff}$	log R
10^{-6}	7.84650	0.87274	6.08715	4.84250	11.72763
10^{-7}	7.92150	1.09791	6.09132	4.88074	11.65323
10^{-8}	8.00027	1.33451	6.09652	4.92088	11.57558
10^{-9}	8.08323	1.58381	6.10314	4.96315	11.49433
10^{-10}	8.17087	1.84730	6.11174	5.00775	11.40942

As a result of their high mass and temperature, very massive stars are dominated by radiation pressure and they have luminosities closer to the Eddington limit. The specific luminosity $L_\nu \sim L_{\rm Edd} \sim M$, and the total luminosity depends on the total mass of stars only but it is independent of the IMF (Bromm et al. 2001), which is a unique characteristic of very massive stars.

Mass loss can affect the stellar evolution in a variety of ways. In the present work, nuclear lifetimes for mass losing stars with a mass loss parameter $N = 50$ are similar to those in the conservative case.

Hydrogen and helium burning lifetimes are decreasing with increasing stellar mass. On the other hand, the nuclear lifetimes are increasing with increasing mass loss rates. Nuclear lifetimes also are different depending on the initial chemical composition of the stars. For $M \geq 100\,M_\odot$ galactic and pregalactic Population III stars the nuclear lifetimes during the hydrogen burning are $\tau_{\rm H} \leq 3 \times 10^6$ years. The helium burning lifetimes are shorter than the hydrogen burning lifetimes.

As discussed in Section 2, it is still an open question if the lower metallicity stars could have lost a substantial part of their mass and which could be the mechanisms. We argue that a mass loss is necessary to have a good mixing and transport of the produced elements to the surface of the star. In the conservative case, without any mass loss, the mixing is very deficient and the CNO elements are not transported to the surface. However, in a scenario with mass loss, the mixing is very efficient. The main result is a production of N^{14}, which originates primarily in the pregalactic stars, and subsequently in the galactic ones (Bahena 2006), as it will be shown in details in a forthcoming paper.

Meynet and Maeder (2002) and Maeder and Meynet (2003) have shown that the stellar rotation and mass loss can affect the predictions of the stellar yields especially for He, C, N and O. At low Z, the rotation may be a dominant effect in massive star evolution. They estimate that low Z stars may loose mass due to fast rotation as a consequence of their initial slow winds, and initial rotation velocities may be faster (Maeder et al. 1999). Their models of massive stars at low Z do not reach in general the red stage. However, rotation permits the envelope to largely expand and the star moves to the red supergiant stage, modifying all the models outputs. Then, the rotation affects the evolution of very metal-poor massive stars (Meynet et al. 2005) and can induce mass loss in many ways (Meynet et al. 2006a). The compactness of low metallicity stars is a key property which has many effects in relation with stellar rotation.

For the present work, Tables 2 and 3 indicate some features for galactic and pregalactic Population III mass losing stars. The first column lists the initial stellar mass M_i, the second one refers to the mass loss parameter N. The next columns indicate the lifetime $\tau_{\rm H}$ during hydrogen burning given in Mega-years, the mass ejecta during the hydrogen burning $\Delta M_{\rm H}$, the convective core size $q_{\rm cc,\,H}$ during this phase and the corresponding He-core mass $M_{\rm He}$. Then there follow the lifetime $\tau_{\rm He}$ during helium burning in Mega-years, the convective core size $q_{\rm cc,\,He}$ during this burning phase and the CO-core mass $M_{\rm CO}$. The mass ejecta, the He- and CO-core masses are given in solar masses.

In our models the mass ejecta are important during hydrogen burning and they increase with increasing initial stellar mass. For 100 and 200 $M_\odot$ pregalactic stars, with $N = 100$, the ejecta $\Delta M_{\rm H}$ are 26.82 and 59.08 $M_\odot$, respectively.

In the present work, mass losing stars form a convective core size slightly greater than in the conservative case. Stars evolving with mass loss parameter $N = 100$ form a helium core $M_{\rm He} = 32.98$, and 71.27 $M_\odot$ for 100

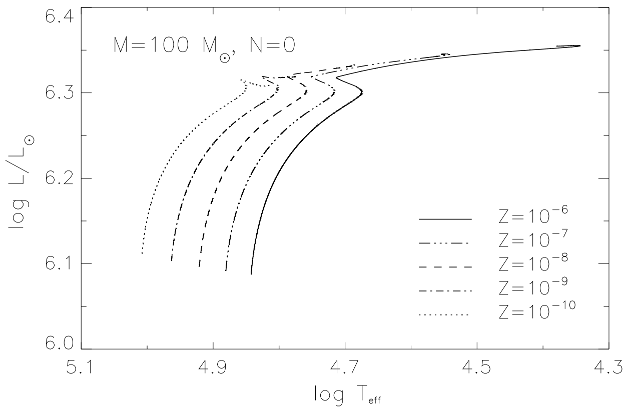

Fig. 17 Evolutionary tracks in the HR-diagram for a $100 M_\odot$ stars with different low-metallicity at constant mass. The lower is the metallicity the bluer are the loci of the stars.

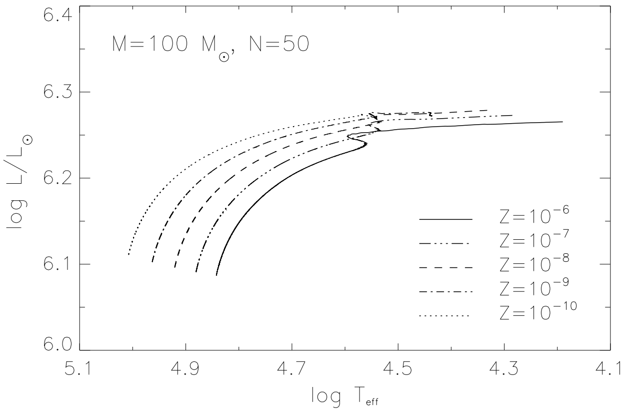

Fig. 18 Idem dito. Evolutionary tracks in the HR-diagram for a $100 M_\odot$ stars with different low-metallicity for mass losing stars by using a mass loss parameter $N = 50$.

Table 2 Nuclear life times and masses during hydrogen and helium burning for 100, 120, 150, 200 and 250 $M_\odot$ galactic Population III stars with initial metallicity $Z = 10^{-6}$, and diverse mass loss parameters.

$M_{\rm i}$	N	$\tau_{\rm H}$	$\Delta M_{\rm H}$	$q_{\rm cc,H}$	$M_{\rm f,H}$	$M_{\rm He}$	$\tau_{\rm He}$	$q_{\rm cc,He}$	$M_{\rm f,He}$	$M_{\rm CO}$
100	0	3.09834	0.00000	0.41562	100.00000	41.56200	3.14857	0.38515	100.00000	38.51500
	50	3.07066	14.64268	0.45946	85.35732	39.21827	3.07857	0.33416	85.30596	28.50584
	100	3.15136	26.82291	0.45071	73.17709	32.98165	3.15890	0.30761	73.09620	22.48512
120	0	2.89075	0.00000	0.43025	120.00000	51.64200	2.93901	0.40415	120.00000	48.49800
	50	2.87198	17.78249	0.47813	102.21751	48.87326	2.87981	0.33142	102.21992	33.87773
	100	2.94026	32.84446	0.47004	87.15554	40.96659	2.94880	0.34399	87.04112	29.94127
150	0	2.67959	0.00000	0.44097	150.00000	66.14550	2.72591	0.42386	150.00000	63.57900
	50	2.67557	23.56230	0.49297	126.43770	62.32999	2.68253	0.38855	126.42807	49.12363
	100	2.73644	43.49372	0.49057	106.50628	52.50440	2.74280	0.38651	106.33505	41.09956
200	0	2.46549	0.00000	0.45237	200.00000	90.47400	2.50979	0.42152	200.00000	84.30400
	50	2.43380	32.71329	0.50490	167.28671	84.46306	2.48056	0.37267	167.27864	62.33973
	100	2.51988	59.07631	0.50571	140.92369	71.26652	2.52582	0.34120	140.68414	48.00143
250	0	2.32990	0.00000	0.46402	250.00000	116.00500	2.37348	0.45782	250.00000	114.45500
	50	2.34590	41.44418	0.51272	208.55582	106.00500	2.35321	0.40578	208.37607	84.55484
	100	2.38727	45.41756	0.51194	174.58244	89.37573	2.39382	0.41550	174.27963	72.41319

and 200 $M_\odot$ galactic ($Z = 10^{-6}$) stars, respectively. For pregalactic ($Z = 10^{-9}$) stars, $M_{\rm He} = 32.29$ and 68.72 $M_\odot$, respectively. The corresponding carbon core masses are 22.48 and 48.00 $M_\odot$ for the first case, and 32.13 and 70.24 $M_\odot$ for the second one, respectively.

Studies of core-collapse SNe have discovered two distinct types of supernovae explosions: (i) very energetic SNe or hypernovae (HNe), and (ii) very faint and low energy SNe. In Nomoto et al. (2004) it was proposed that the first generation supernovae were the explosions of $\sim 20 - 30\,M_\odot$ stars and some of them produced C-rich, Fe poor ejecta. The ejecta of these explosions can well account for the abundance pattern of EMP stars. In contrast, the observed abundance patterns cannot be explained by the explosions of more massive, $130 - 300\,M_\odot$ stars. These stars undergo pair-instability SNe explosions and are disrupted completely (Umeda and Nomoto 2002; Heger and Woosley 2002).

If all stars evolve with mass loss they can reduce their initial mass to massive stars range, as our models show. Depending of their initial mass and mass loss rate, its final fate could be either SNe or HNe. The HNe explosions connected to some low-z gamma-ray bursts could be relevant to early nucleosynthesis at low metallicity (Umeda and Nomoto 2002).

5 Conclusions

The main aim of the present study was to construct models for very massive low-metallicity both galactic and pregalactic Population III mass losing stars. We have calculated and discussed here the main properties of these stars in comparison with the conservative case presented in Paper I. Our results show that the mass loss could be very important for massive low metallicity stars, although the physics and mechanisms of the mass loss are not well known yet. According to the line-driven wind theory, the mass loss rate is negligible for the very low metallicity. However, the mass loss may occur due to other processes which are metallicity independent, such as effects of continuum radiation, pulsation and/or rotation etc. In our approach we have chosen an ad hoc rate of the mass loss and we used the know physics to explore its effects on the stellar evolution at very low Z.

For evolution with mass loss, the reduction of the stellar mass makes the central temperature to increase less rapidly than for constant-mass evolution. Thus the mass of the convective core decreases more rapidly as the evolution proceeds. However, the core mass fraction is larger in a star evolving with mass loss. The luminosity of a star evolving with mass loss is lower than for constant-mass evolution and in consequence its main-sequence lifetime is somewhat increased.

The evolution of VMS both with and without mass loss takes place in the upper part of the HR-diagram. In the absence of heavy CNO elements, lower metallicity galactic and pregalactic stars contract and settle down on the ZAMS with central temperatures high enough for some ^{4}He to be converted to CNO nuclides through the triple-α reaction and CNO cycles. The energy generated stops the contraction and the star re-expands.

Table 3 Nuclear life times and masses during hydrogen and helium burning for 100, 120, 150, 200 and 250 $M_\odot$ pregalactic Population III stars with initial metallicity $Z = 10^{-9}$, and diverse mass loss parameters.

M_i	N	τ_H	ΔM_H	$q_\mathrm{cc,H}$	$M_\mathrm{f,H}$	M_He	τ_He	$q_\mathrm{cc,He}$	$M_\mathrm{f,He}$	M_CO
100	0	2.89133	0.00000	0.37951	100.00000	37.95100	2.93547	0.38910	100.00000	38.91000
	50	2.89685	14.31142	0.44794	85.68958	38.38334	2.93011	0.44891	85.39561	38.33494
	100	2.95916	26.23277	0.43772	73.76723	32.28939	2.97677	0.43679	73.55861	32.12967
120	0	2.69832	0.00000	0.38496	120.00000	46.19520	2.73923	0.40604	120.00000	48.72480
	50	2.70386	17.72365	0.46846	102.27635	47.91238	2.74578	0.46763	102.26871	47.82392
	100	2.76936	32.99806	0.46448	87.00194	40.41066	2.81274	0.46295	86.43422	40.01472
150	0	2.50358	0.00000	0.39613	150.00000	59.41950	2.54207	0.41884	150.00000	62.82600
	50	2.52162	22.89308	0.48177	127.10692	61.23630	2.52587	0.49071	127.09890	62.36826
	100	2.57387	41.94500	0.47805	108.05500	51.65569	2.57775	0.49219	108.04709	53.17970
200	0	2.30257	0.00000	0.41782	200.00000	83.56400	2.34043	0.43612	200.00000	87.22400
	50	2.34086	31.96341	0.48552	168.03659	81.58513	2.34750	0.48872	168.02637	82.11785
	100	2.38205	58.43802	0.48546	141.56198	68.72268	2.38542	0.49668	141.41945	70.24021
250	0	2.17765	0.00000	0.42354	250.00000	105.88500	2.21375	0.44310	250.00000	110.77500
	50	2.22612	40.76518	0.48886	209.23482	102.28653	2.23255	0.49352	209.16652	103.22786
	100	2.25313	74.29857	0.48770	175.70143	85.68959	2.25955	0.49271	175.39363	86.41820

In all cases, lower metallicity pushes the stars to a smaller radius at higher density and temperature. Therefore, galactic and pregalactic Population III stars are more compact, hotter and denser than their metal enriched counterparts. Due to their different chemical composition, the luminosity is slightly lower for pregalactic stars.

The evolution of both galactic and pregalactic Population III stars is influenced by the increase of the mean molecular weight in the convective core and the effect of mass loss. The mean molecular weight affects the star by increasing their luminosity. As a result of the increased mean molecular weight in the convective core the central temperature also increases. With increased molecular weight the convective core shrinks. The contraction of the convective core makes the star to expand and the effective temperature to decrease. The proportionality between mass and luminosity causes that the luminosity decreases as the star loses mass.

Heger and Woosley (2002) and Heger et al. (2002, 2003) have studied the final fate of VMS considering only the conservative evolution. Stars with $140\,M_\odot < M < 260\,M_\odot$ explode as Pair-Instability Supernovae Explosions (PISNe) causing complete disruption. In these cases, $M_\mathrm{He} \sim 64 - 133\,M_\odot$.

Our models for $200\,M_\odot$ galactic and pregalactic stars develop in the conservative case $M_\mathrm{He} \sim 90$ and $84\,M_\odot$, respectively. With moderate mass loss rate ($N = 50$), they develop $M_\mathrm{He} \sim 84$, and $82\,M_\odot$. With increasing mass loss rate ($N = 100$), stars develop $M_\mathrm{He} = 71$ and $69\,M_\odot$. Then, these galactic and pregalactic stars could explode as PISNe.

However, according to scenarios by Umeda and Nomoto (2002, 2003); Umeda et al. (2002); Nomoto et al. (2004), the stars with $M < 130\,M_\odot$ could explode like HNe. Our $100\,M_\odot$ galactic and pregalactic models develop $M_\mathrm{He} \sim 42$ and $38\,M_\odot$ in the conservative case ($N = 0$), $M_\mathrm{He} \sim 39$ and $38\,M_\odot$ with a moderate mass loss rate ($N = 50$), and with $N = 100$, they have $M_\mathrm{He} = 33$ and $32\,M_\odot$, respectively. Then, models for $\leq 100\,M_\odot$ mass losing stars, which evolve with high mass loss rates, can reduce appreciably their initial mass during the hydrogen, and helium burning. Their cores could also explode like HNe, which are likely to make an important contribution to the early galactic chemical evolution.

The most important effect in the transition in the star formation properties from the first stars to present day is the presence of a trace amount of heavy elements. The concept of critical metallicity has been used to characterize the transition between Population III and Population II star formation modes (Omukai 2001; Bromm et al. 2001; Bromm and Larson 2004). This important parameter value of critical threshold for enabling a formation of stars with lower mass is estimated to be $Z \sim 10^{-3.5} Z_\odot \sim 6.32 \times 10^{-6}$. In our very massive evolutionary models, their initial mass is reduced when they lost mass reaching the range of massive stars. Due to the mass loss an efficient mixing of CNO elements is reached. After hydrogen burning, the initial metallicity increases providing an initial enrichment of the IGM with heavy elements, giving place to the next generation of stars with increasing metallicity. In successive generations the EMP stars observed in present days could be formed.

The evolution of the first stars with mass loss is still an open problem. It would be interesting to suppose that the rotation or other mechanisms driving the mass loss is simultaneously responsible for a mixing of elements in the stellar interiors. The main problem, however, is to find a realistic model for the mass loss rate due to the different mechanisms and their combinations and to include it into self-consistent models of the stellar evolution.

This work has been partially supported by the Mexican Consejo Nacional de Ciencia y Tecnología (CONACyT). DB thanks to CONACyT for a Ph. D. grant, P.H. acknowledges grants LC0614 and 202/09/0772.

References

Abel T., Bryan G.L., Norman M.L.: Science **295**, 93 (2002).

Bahena D.: PhD Thesis, UK, Praha (2006).

Bahena D., Klapp J.: Astrophys. Sp. Sci., **53** 327, 219 (2010). Paper I.

Baraffe I., Heger A., Woosley S.E.: Astrophys. J., **550**, 890 (2001).

Barlow M.J., Cohen M.: Astrophys. J., **213**, 737 (1977).

Beers T.C., Christlieb N.: Annu. Rev. Astron. Astrophys., **43**, 531 (2005).

Bromm V., Kudritzki R.P., Loeb A.: Astrophys. J., **552**, 464 (2001).

Bromm V., Loeb A.: Nature, **425**, 812 (2003).

Bromm V., Larson R.B.: Annu. Rev. Astron. Astrophys., **42**, 79 (2004).

Cassisi S., Castellani V.: Astrophys. J. Suppl. Ser., **88**, 509 (1993).

Castellani V.: In *The First Stars*, Proc. of the MPA/ESO Workshop held at Garching, 4-6 august 1999, A. Weiss, T. Abel, V, Hill (eds.), Springer, p. 85 (2000)

Castor J.I., Abbott D.C., Klein R.I.: Astrophys. J., **195**, 157 (1975).

Cescutti G., Chiappini C.: Astron. Astrophys., **515**, A102 (2010).

Dwarkadas V.V., Owocki S.P.: Astrophys. J., **581**, 1337 (2002).

Gräfener G., Hamann E.-R.: Astron. Astrophys., **482**, 945 (2008).

Heger A., Woosley S.E.: Astrophys. J., **567**, 532 (2002).

Heger A., Woosley S.E., Baraffe I., Abel T.: In *The Most Luminous Celestial Objects and Their Use for Cosmology*, Proc. MPA/ESO/MPE/USM, eds. M. Gilfanov, R. Sunyaev and E. Churazov, Springer, p.369 (2002).

Heger A., Fryer C., Woosley S.E., Langer N., Hartmann D.H.: Astrophys. J., **591**, 288 (2003).

Hirschi R., Chiappini C., Meynet G., Maeder A., Ekström S.: In *Massive Stars and Cosmic Engines*, F. Bresolin, Crowther P.A., and Puls J. (eds.), Proc. IAU Symp. **250**, p. 217 (2007)

Klapp J., Bahena D., Corona-Galindo M.G. et al.: In: *Gravitation and Cosmology*, A. Macías, C. Lämmerzahl and D. Nuñez (eds.), Melville N.Y., AIP Conf. Proc. **758**, p. 153 (2005).

Krtička J., Kubát J.: Astron. Astrophys., **446**, 1039 (2006).

Krtička J., Kubát J.: Astron. Astrophys., **493**, 585 (2009).

Krtička J., Owocki S. P., Meynet G.: In *Chemical Abundances in the Universe: Connecting First Stars to planets*, Cunha K., Spite M., and Barbuy B. (eds.), Proc. IAU Symp. **265**, p. 69 (2010a)

Krtička J., Votruba V., Kubát J.: Astron. Astrophys., **516**, 100 (2010b).

Krtička J., Owocki S. P., Meynet G.: Astron. Astrophys., **527**, 84 (2011).

Kudritzki R.P.: Astrophys. J., **577**, 389 (2002).

Lamers H.J.G.L.M., Snow T.P., Lindholm D.M.: Astrophys. J., **455**, 269 (1995).

Leitherer C., Robert R., Drissen L.: Astrophys. J., **401**, 596 (1992).

Lucy L.B., Solomon P.M.: Astrophys. J., **159**, 879 (1970).

Mackey J., Bromm V., Hernquist L.: Astrophys. J., **586**, 1 (2003).

Maeder A.: In *Boulder-Munich III: properties of Hot, Luminous Stars*, Ian D. Howarth (ed.), ASP Conf. Ser., **131**, 85 (1998).

Maeder A., Grebel E.K., Mermilliod J.-C.: Astron. Astrophys., **346**, 459 (1999).

Maeder A., Desjacques V.: Astron. Astrophys., **372**, L9 (2001).

Maeder A., Meynet G.: Astron. Astrophys., **373**, 555 (2001).

Maeder A., Meynet G.: In: *Stellar Rotation*, Proc. IAU Symp. **215**, A. Maeder and P. Eenens (eds.), p. 500 (2003).

Meynet G., Maeder A.: Astron. Astrophys., **321**, 465 (1997).

Meynet G., Maeder A.: Astron. Astrophys., **361**, 101 (2000).

Meynet G., Maeder A.: Astron. Astrophys., **390**, 561 (2002).

Meynet G., Maeder A., Ekström S.: In *The Fate of the Most Massive Stars*, R. Humphreys and K. Stanek (eds.), ASP Conf. Ser. **332**, p. 228 (2005).

Meynet G., Hirschi R., Ekström S., Maeder A.: In *Stellar Evolution at Low Metallicity¿ Mass Loss, Explosions, Cosmology*, Lamers H.J.G.L.M., Langer N., Nugis T. and Kalju A. (eds.), ASP Conf. Ser. **353**, p. 49 (2006a).

Meynet G., Maeder A., Hirschi R. et al.: In *Int. Symp. Nuc. Astrophys., Nuclei in the Cosmos-IX*, Proc. of Sci., CERN, p.1 (200b).

Nakamura F., Umemura M.: Astrophys. J., **548**, 19 (2001).

Nakamura T., Umeda H., Nomoto K. et al.: Astrophys. J., **517**, 193 (1999).

Nomoto K., Maeda K., Umeda H. et al.: Mem. S.A. It. **75**, 312 (2004).

Omukai K.: Astrophys. J., **546**, 635 (2001).

Omukai K., Palla P.: Astrophys. J., **589**, 677 (2003).

Puls J., Vink J.S., Najarro F.: Astron Astrophys Rev., **16**, 209 (2008)

Reimers D.: Mem. Soc. R. Sci. Liège, **8**, 369 (1975)

Reimers D.: Astron. Astrophys., **61**, 217 (1977).

Schneider R., Ferrara A., Natarajan P., Omukai K.: Astrophys. J., **571**, 30 (2002).

Schneider R., Ferrara A., Salvaterra R., Bromm V.: Nature, **422**, 869 (2003).

Schröder K.P., Cuntz M.: Astrophys. J., **630**, L73 (2005).

Smith N., Owocki S. P.: Astrophys. J., **645**, L45 (2006)

Stacy A., Bromm V., Loeb A.: Mon. Not. R. Astron. Soc., **413**, 543 (2011)

Tumlinson J., Venkatesan A., Shull M.J.: Astrophys. J., **612**, 602 (2004).

ud-Doula A., Owocki S.P., Towsend H.D.: Mon. Not. R. Astron. Soc., **385**, 97 (2008)

Umeda H., Nomoto K.: Astrophys. J., **565**, 385 (2002).

Umeda H., Nomoto K.: Nature **422**, 871 (2003).

Umeda H., Nomoto K., Tsuru T.G., Matsumoto H.: Astrophys. J., **578**, 885 (2002)

van Marle A.J., Owocki S.P., Shaviv N.J.: In *First Stars III: First Stars II Conf.*, AIP Conf. Proc., **900**, p. 250 (2008a).

van Marle A.J., Owocki S.P., Shaviv N.J.: Mon. Not. R. Astron. Soc., **389**, 1353 (2008b).

Vink J.S., de Koter A., Lamers H.J.G.L.M.: Astron. Astrophys., **350**, 181 (1999).

Vink J.S., de Koter A., Lamers H.J.G.L.M.: Astron. Astrophys., **362**, 295 (2000).

Vink J.S., de Koter A., Lamers H.J.G.L.M.: Astron. Astrophys., **369**, 574 (2001).

Vink J.S., Muijres L.E., Anthonisse B. et al.: Astron. Astrophys., **531**, 132 (2011).

This manuscript was prepared with the AAS LATEX macros v5.2.